

RSC Advances



This is an *Accepted Manuscript*, which has been through the Royal Society of Chemistry peer review process and has been accepted for publication.

Accepted Manuscripts are published online shortly after acceptance, before technical editing, formatting and proof reading. Using this free service, authors can make their results available to the community, in citable form, before we publish the edited article. This *Accepted Manuscript* will be replaced by the edited, formatted and paginated article as soon as this is available.

You can find more information about *Accepted Manuscripts* in the [Information for Authors](#).

Please note that technical editing may introduce minor changes to the text and/or graphics, which may alter content. The journal's standard [Terms & Conditions](#) and the [Ethical guidelines](#) still apply. In no event shall the Royal Society of Chemistry be held responsible for any errors or omissions in this *Accepted Manuscript* or any consequences arising from the use of any information it contains.

Cite this: DOI: 10.1039/c0xx00000x

www.rsc.org/xxxxxx

ARTICLE TYPE

Designing Bodipy-Based Probes for Fluorescence Imaging of β -amyloid Plaques

Fazli Sozmen,^{‡a} Safacan Kolemen,^{‡a} Henri-Obadja Kumada,^b Masahiro Ono,^b Hideo Saji^b and Engin U. Akkaya^{*ac}

Received (in XXX, XXX) Xth XXXXXXXXX 20XX, Accepted Xth XXXXXXXXX 20XX
DOI: 10.1039/b000000x

Styryl-conjugated Bodipy dyes which are structurally similar to known $A\beta$ peptide binding dyes, were designed and synthesized. The binding is accompanied by large increase in the emission intensity in all cases, suggesting a high potential for use in the fluorescence imaging of $A\beta$ plaques.

Introduction

Alzheimer's disease (AD) is an important neurological disorder that affects mostly the elderly by diminishing the quality of life to a drastic extent.¹ It is under study worldwide as it is considered to be one of the most important diseases. Nevertheless, an effective treatment remains elusive. Today, more than 24 million people have been affected by AD worldwide and it is estimated that number will reach 100 million people by 2050.^{1e,2} Considering the lack of a cure, early detection and monitoring are therefore very significant for satisfactorily managing this disease. Accurate diagnosis rests on the detection of β -Amyloid ($A\beta$) plaques since the progression of disease is linked to the appearance and accumulation of these plaques.³ $A\beta$ plaques are formed by the amyloid precursor proteins (APP) which are mainly composed of $A\beta$ 40 and $A\beta$ 42(43) peptides that are deposited early, and most likely, selectively in the senile plaques following cleavage with β - (BACE) and γ - secretases.⁴ These plaques may play a role in other neurodegenerative diseases such as Creutzfeldt-Jakob and carpal tunnel syndrome, it is also possible to observe $A\beta$ plaques formation in the brains of the patients with those diseases. $A\beta$ 40 and $A\beta$ 42 are known to be the main amyloid peptides in humans. Although $A\beta$ 40 is more abundant one, $A\beta$ 42 forms aggregates more rapidly.⁵ It is thought that, free radicals result in oxidative stress, which play important role in protein metabolism, may be the major reason for the $A\beta$ aggregation.⁶

Positron emission tomography⁷ (PET) and magnetic resonance imaging⁸ (MRI) are widely used conventional techniques for diagnosis of AD. Sensitivity, cost and maintenance problems of the devices are the major drawbacks associated with these methods. On the other hand, near-IR fluorescence imaging technique offers noninvasive, simple and inexpensive detection tool for the $A\beta$ plaques.^{9,10} Thus fluorescence imaging can be a good alternative to conventional techniques if probes can be

designed according to special requirements. Primary requirement for a probe is that its high affinity towards $A\beta$ plaques. In addition to that, the probe compound should have lipophilic character and its molecular weight should be less than 600 Da in order to pass through the blood brain barrier efficiently.¹⁰ Moreover, it should be stable in the physiological medium with no or weak interaction with the serum components. Finally, probe has to be emissive at longer wavelengths (in order to overcome the limitations imposed by the low penetration depth of the light) of the electromagnetic spectrum upon binding to $A\beta$ plaques.

BODIPY derivatives, especially for the last decade have been proposed for applications in many diverse areas such as molecular sensors/logic gates,¹¹ photodynamic therapy,¹² dye sensitized solar cells¹³ and light harvesting/energy transfer cassettes.¹⁴ This, among other reasons is most likely due to their suitable characteristics such as high absorption coefficient, easy synthesis, multiple modification sites and high fluorescence quantum yields. As this class of compounds can be transformed into long wavelength absorbing and emitting dyes¹⁵ they also have significant potential in imaging in biological milieu, as near-IR fluorophores have definite advantages over fluorophores that operate in the visible region, such as lower auto-fluorescence/scattering and deeper penetration of the exciting light through tissues for biomedical applications. Synthetically, the most attractive property of BODIPY dyes is their rich chemistry and easy derivatization at every position on the core. For instance, sequential Knoevenagel condensation reactions can be utilized to synthesize styryl-BODIPY derivatives enabling the tuning of the absorption band of BODIPY dyes within the range of 500-900 nm. The condensation reactions on the BODIPY core make use of the acidic methyl substituents on the Bodipy core.¹⁶ Even though not frequently explored in such reactions, the methyl group at the *meso*-positions would also be acidic enough to deprotonate and undergo condensation reactions with various aldehydes. In consideration of the rich chemistry of Bodipy dyes and apparent requirements for $A\beta$ plaques detection into account, we targeted the synthesis of a series of BODIPY based near-IR imaging probes for $A\beta$ plaques.

The principle idea is as follows: The structures of the thioflavin T used for visualizing $A\beta$ plaques in the brain, and that of the PET probes demonstrated to be valuable for *in vivo*

imaging amyloid aggregates are shown below (Figure 1). Certain structural features become apparent. Aminophenylethenyl unit is a recurring theme. With that starting point and constraining ourselves with the molecular weight and lipophilicity (ideally, 2.5 in consideration of the blood-brain barrier), we proposed the following target compounds (EUA1–5) shown in scheme 1 as potential candidates for fluorescent imaging.

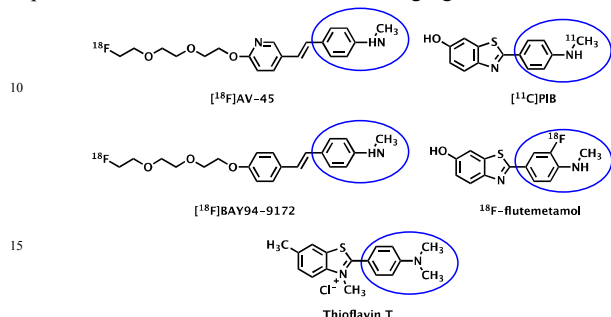
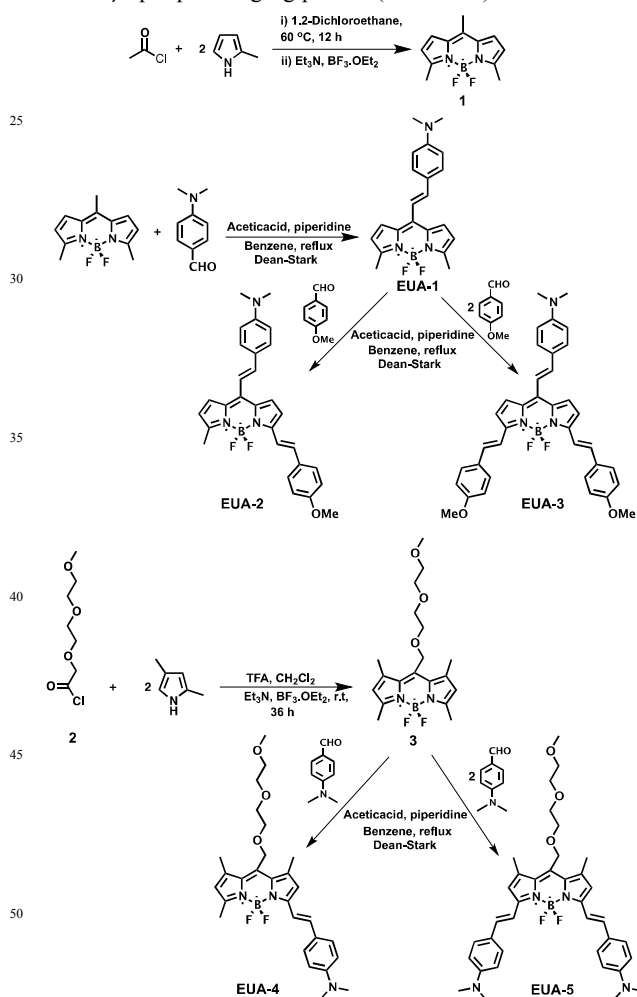


Figure 1. The structures of common PET probes and thioflavin T stain, which are used for the detection of A β plaques in the brain.

Results and discussion

We specifically targeted and synthesized five new BODIPY based A β plaque imaging probes (EUA-1–5) which have



Scheme 1. The synthesis of β -Amyloid imaging probes EUA-1–5.

55 different affinities for A β aggregates. In our design, probes can be grouped into two sets; in the first set (EUA-1–3), the dimethylaminostyryl groups, which have known affinity to A β plaques, are placed at the *meso* position of the Bodipy core, and in the second one, the dimethylaminostyryl groups are at the 3- and 5- positions of Bodipy core. Moreover, the second set of probes (EUA-4 and 5) include triethyleneglycole moieties in order to make them more compatible within the biological medium with enhanced water and lipid solubility.

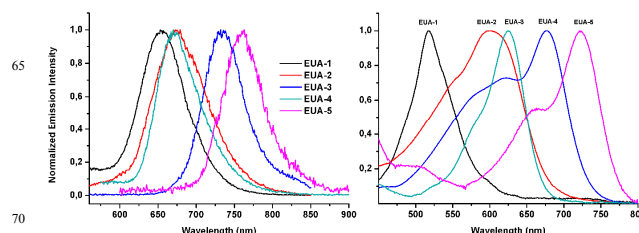


Figure 2. Normalized electronic absorption and emission spectra of EUA-1 through EUA-5 probes in CHCl₃.

To these ends, we first synthesized **1** according to well-known protocol which involves the reaction between acetyl chloride and 2-methylpyrrole. Then the Knoevenagel condensation reaction between **1** and 4-(N,N-dimethylamino)benzaldehyde yielded **EUA-1**. In this reaction, condensation takes place preferentially at the methyl groups positioned on the *meso* carbon of the parent dye, as reported previously in the literature. The others in the set were also obtained by applying a series of Knoevenagel reactions with 4-methoxybenzaldehyde (compounds **EUA-2&3**).

In order to synthesize the other two probes **EUA-4** and **EUA-5**, first compound **3** was prepared by the reaction of 2-methyl-pyrrole and 2-(2-(2-methoxyethoxy)ethoxy)acetyl chloride (**2**) which is obtained by Jones oxidation of triethyleneglycol methyl ether. Finally, **EUA-4** and **EUA-5** were obtained simply as products following Knoevenagel condensation reactions with 4-(dimethylamino)benzaldehyde and the compound **3**.

The fluorescence and electronic absorption properties (Figure 2) of these compounds were acquired in chloroform and the selected data are presented in table 1. Probes having styryl groups possess longer wavelength absorption and emission maxima, due to the extension of π -conjugation in these compounds.

Table 1. Photophysical characterization of probes.

| Probes | λ_{abs} (nm) ^a | ϵ (M ⁻¹ cm ⁻¹) | λ_{ems} (nm) ^a | Φ_{F} (%) | τ (ns) ^a |
|--------|--|--|--|-----------------------|--------------------------|
| EUA-1 | 518 | 46000 | 654 | 12 ^b | 1.98 |
| EUA-2 | 597 | 72000 | 667 | 7 ^c | 1.40 |
| EUA-3 | 677 | 66000 | 736 | 1 ^d | 0.74 |
| EUA-4 | 624 | 85000 | 673 | 13 ^d | 0.42 |
| EUA-5 | 721 | 81000 | 763 | 3 ^d | 1.08 |

^aData acquired in chloroform, In reference to ^bRhodamine 6G in H₂O ($\lambda_{\text{exc}} = 488$ nm, $\Phi_{\text{F}} = 95\%$), ^cSulphorodamine in ethanol ($\lambda_{\text{exc}} = 550$ nm, $\Phi_{\text{F}} = 90\%$), ^dCrystal Violet in methanol ($\lambda_{\text{exc}} = 610$ nm, $\Phi_{\text{F}} = 66\%$).

Absorption spectra of probes in chloroform show typical styryl BODIPY bands ($S_0 \rightarrow S_1$) which are in the so-called therapeutic window (600-900 nm), suggesting a likelihood of *in vivo* potential. As expected, the fluorescence quantum yields of these compounds are lower. However, upon binding to plaques fluorescence intensity is enhanced as shown in $A\beta$ saturation curves (Figure 3) and cell culture studies (Figure 4A).

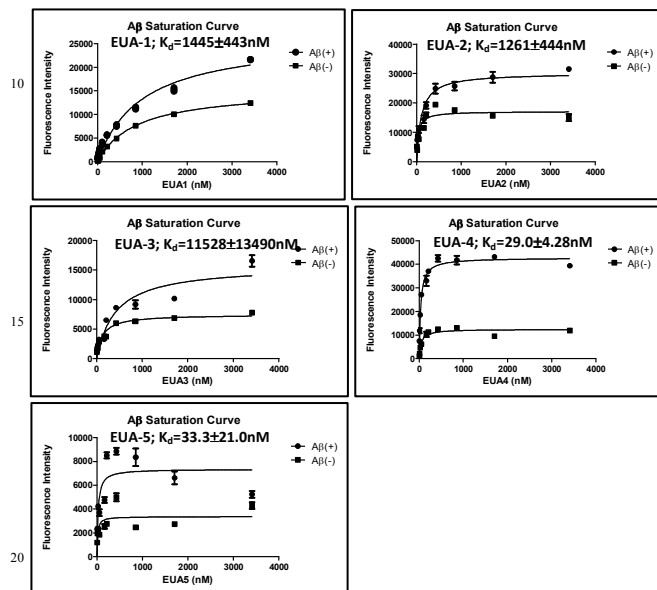


Figure 3. Plot of the fluorescence intensity ($\lambda_{em} = 680, 744, 720, 698,$ and 784 nm for **EUA-1**, **EUA-2**, **EUA-3**, **EUA-4**, and **EUA-5**, respectively) as a function of the concentration of **EUA-1–5** in the presence of $A\beta$ aggregates (2.2 μ M) in solutions.

The dissociation constants (K_d) of the probes **EUA1–5** were determined through saturation curves of β -Amyloid plaques which are obtained by plotting the fluorescence intensities against probe concentration graphs (Scatchard plots, Figure 3).

The dissociation constants of **EUA1–5** are 1400 ± 400 nM, 1300 ± 400 nM, 11500 ± 13000 nM, 29.0 ± 4.0 nM and 30.0 ± 20.0 nM, respectively. All probes showed different binding affinities, however **EUA-4** and **EUA-5** have much lower K_d values indicating that these probes have extremely high affinities to $A\beta$ plaques, especially **EUA-4** is better than most of the approved PET probes. The difference in emission intensities do not correlate with the K_d values, which is not surprising considering an enhanced quantum yield may depend on a number of microenvironmental parameters, in addition to the actual structure of the probe.

The lipophilicity ($\log P$), which is very important for *in vivo* studies and in principle, can be easily adjusted via substitution (such as attaching alkyl chains), was measured for **EUA1–5** and found as 6.3, 5.9, 5.9, 5.8 and 4.9 respectively (ESI). Brain sections of Tg2576 mice (transgenic mice which carries an early-onset gene, typically used for modeling AD) which particularly produce $A\beta$ plaques were used to evaluate the binding of probes to $A\beta$ plaques *in vitro* experimentally. Lots of fluorescent spots were shown in the

brain sections of Tg2576 (female, 28-months-old) mice (Figure 4A). In order to confirm the affinity of probes, thioflavin S was used to stain $A\beta$ plaques as a conformation dye (Figure 4B). The staining patterns demonstrated the particular binding of dyes. Among the probes, **EUA-3** which has the weakest affinity, and it did not show an appreciable staining patterns in the brain sections from Tg2576 mouse. On the other hand the **EUA-1**, **EUA-2** and **EUA-4** stained the brain sections efficiently and demonstrated good patterns. Even though the **EUA-5** has very small K_d value, staining is not pronounced as in the case of **EUA-1**, **EUA-2** and **EUA-4**. The **EUA-4** with smallest K_d value stained the brain sections best.

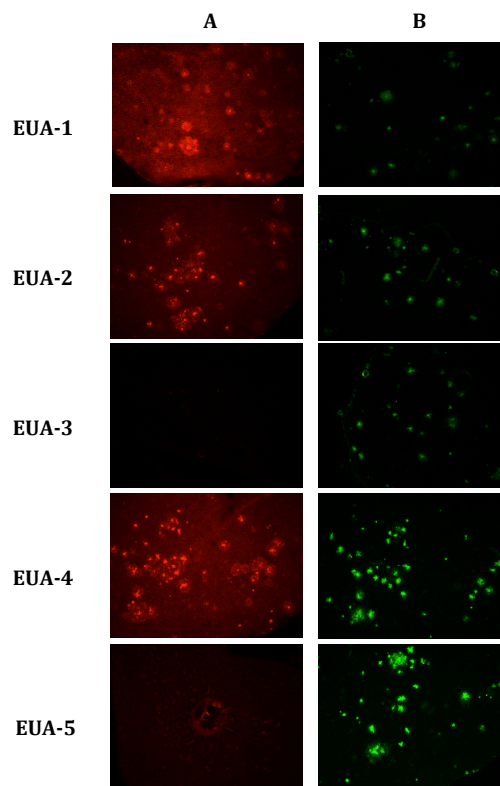


Figure 4. (A) Neuropathological staining of **EUA1–5** in a 10- μ m section from Tg2576 mice brains (female, 28-months-old). (B) Labeled plaques were confirmed by staining of the adjacent section with thioflavin-S.

Conclusion

In conclusion, five new potential fluorescent probes for $A\beta$ plaques were developed which operate in the longer wavelength region of the visible spectrum. Among these probes **EUA-1**, **EUA-2** and **EUA-4** showed considerably good staining patterns in the brain sections from Tg2576 mice. Especially, the **EUA-4** that possesses the highest affinity and better fluorescence imaging characteristics seems very promising. Further derivatization, targeting near-IR emission and reduced polarity should yield improved compounds with highly desirable emission properties. Work along that line is in progress.

Experimental section

General

All chemicals and solvents obtained from suppliers were used without further purification. ^1H NMR and ^{13}C NMR spectra were recorded on Bruker Spectrospin Avance DPX 400 spectrometer using CDCl_3 as the solvent. Chemical shifts values are reported in ppm from tetramethylsilane as internal standard. Spin multiplicities are reported as the following: s (singlet), d (doublet), m (multiplet). HRMS data were acquired on an Agilent Technologies 6530 Accurate-Mass Q-TOF LC/MS. UV-Vis Absorption spectra were taken on a Varian Cary-100 and Varian Cary 5000 UV-VIS-NIR absorption spectrophotometer. Fluorescence measurements were done on a Varian Eclipse spectrofluorometer. The Fluorescence decay measurements were carried out with the Horiba Jobin-Yvon Time-Resolved Fluorometer, Fluorolog FL-1057. The instrument response function was measured with an aqueous Ludox solution. Spectrophotometric grade solvents were used for spectroscopy experiments. Flash column chromatography (FCC) was performed by using glass columns with a flash grade silica gel (Merck Silica Gel 60 (40–63 μm)). Reactions were monitored by thin layer chromatography (TLC) using precoated silica gel plates (Merck Silica Gel PF-254), visualized by UV-Vis light. All organic extracts were dehydrated over anhydrous Na_2SO_4 and concentrated by using rotary evaporator before being subjected to FCC.

Synthesis of the compound 1:

To a 1 L round-bottomed flask containing 400 mL argon-degassed 1,2-dichloroethane were added 2-methylpyrrole (8.41 mmol, 1.035 g) and acetyl chloride (3.5 mmol, 1.0 g). The reaction mixture was refluxed overnight at 60°C . 5 mL of Et_3N and 5 mL of $\text{BF}_3\cdot\text{OEt}_2$ were successively added and after 30 min, the reaction mixture was washed three times with water (3 x 100 mL), which was then extracted into the CH_2Cl_2 (3 x 100 mL) and dried over anhydrous Na_2SO_4 . The solvent was evaporated and the residue was purified by silica gel column chromatography using CH_2Cl_2 as the eluent (606.9 mg, 31%). ^1H NMR (400 MHz, CDCl_3): δ 7.05 (d, J = 4.12, 2H), 6.35 (d, J = 4.12, 2H), 2.60 (s, 6H), 2.39 (s, 3H). ^{13}C NMR (100 MHz, CDCl_3): δ 156.7, 140.1, 135.0, 126.9, 122.3, 118.8, 118.7, 118.6, 15.2, 14.7. HRMS: m/z : calcd: 233.1139, found: 233.1100 [M-H] $^-$, Δ =16.8 ppm.

Synthesis of EUA-1:

(1) (0.86 mmol, 200.0 mg) and dimethylaminobenzaldehyde (0.86 mmol, 129.13 mg) were added to a 100 mL round-bottomed flask containing 50 mL benzene and to this solution was added piperidine (0.35 mL) and acetic acid (0.30 mL). The mixture was heated under reflux by using a Dean Stark trap and reaction was monitored by TLC (DCM). When all the starting material had been consumed, the mixture was cooled to room temperature and solvent was evaporated. Water (100 mL) added to the residue and the product was extracted into the CH_2Cl_2 (3 x 100 mL). Organic phase dried over Na_2SO_4 , evaporated and residue was purified by silica gel column chromatography using DCM as the eluent (126 mg, 40%). ^1H NMR (400 MHz, CDCl_3) δ 7.49 (d, J = 8.1 Hz,

2H), 7.38 (d, J = 15.7 Hz, 1H), 7.20 (d, J = 4.0 Hz, 2H), 7.17 (d, J = 15.7 Hz, 1H), 6.73 (d, J = 6.0 Hz, 2H), 6.28 (d, J = 4.0 Hz, 2H), 3.07 (s, 6H), 2.66 (s, 6H). ^{13}C NMR (100 MHz, CDCl_3) δ 154.88, 151.65, 143.77, 140.55, 133.30, 129.52, 126.45, 124.15, 118.02, 117.99, 116.35, 112.02, 40.15, 14.81. HRMS: m/z : calcd: 388.1798, found: 388.1722 [M+Na] $^+$, Δ =19.6 ppm.

Synthesis of EUA-2:

(1) (0.14 mmol, 50.0 mg) and *p*-methoxybenzaldehyde (0.14 mmol, 19.06 mg) were added to a 100 mL round-bottomed flask containing 50 mL benzene and to this solution was added piperidine (0.30 mL) and acetic acid (0.25 mL). The mixture was heated under reflux by using a Dean Stark trap and reaction was monitored by TLC (5% MeOH : 95% DCM). When all the starting material had been consumed, the mixture was cooled to room temperature and solvent was evaporated. Water (100 mL) added to the residue and the product was extracted into the CH_2Cl_2 (3 x 100 mL). Organic phase dried over Na_2SO_4 , evaporated and residue was purified by silica gel column chromatography using (5% MeOH : 95% DCM) as the eluent (20.30 mg, 30%). ^1H NMR (400 MHz, CDCl_3) δ 7.63 (d, J = 16.7 Hz, 1H), 7.58 (d, J = 8.7 Hz, 2H), 7.51 (d, J = 8.8 Hz, 2H), 7.39 (d, J = 15.7 Hz, 1H), 7.30 (d, J = 4.1 Hz, 2H), 7.24 (d, J = 15.5 Hz, 1H), 7.20 (d, J = 4.0 Hz, 1H), 6.94 (m, 3H), 6.74 (d, J = 8.7 Hz, 2H), 6.29 (d, J = 4.0 Hz, 1H), 3.87 (s, 3H), 3.08 (s, 6H), 2.68 (s, 3H). ^{13}C NMR (100 MHz, CDCl_3) δ 160.35, 153.78, 143.05, 138.67, 135.31, 129.58, 129.43, 128.93, 126.64, 125.60, 124.75, 117.76, 117.59, 116.76, 115.00, 114.25, 112.10, 64.62, 55.36, 40.23, 36.51, 31.92, 31.43, 30.31, 30.20, 29.69, 29.65, 29.58, 29.51, 29.35, 29.26, 25.92, 22.68, 14.89, 14.10. HRMS: m/z : calcd: 506.2198, found: 506.3539 [M+Na] $^+$, Δ =0.52 ppm.

Synthesis of EUA-3:

(1) (0.14 mmol, 50.0 mg) and *p*-methoxybenzaldehyde (0.35 mmol, 47.65 mg) were added to a 100 mL round-bottomed flask containing 50 mL benzene and to this solution was added piperidine (0.40 mL) and acetic acid (0.40 mL). The mixture was heated under reflux by using a Dean Stark trap and reaction was monitored by TLC (5% MeOH : 95% DCM). When all the starting material had been consumed, the mixture was cooled to room temperature and solvent was evaporated. Water (100 mL) added to the residue and the product was extracted into the CH_2Cl_2 (3 x 100 mL). Organic phase dried over Na_2SO_4 , evaporated and residue was purified by silica gel column chromatography using (5% MeOH : 95% DCM) as the eluent (25.35 mg, 30%). ^1H NMR (400 MHz, CDCl_3) δ 7.68 (d, J = 16.3 Hz, 2H), 7.62 (d, J = 8.7 Hz, 4H), 7.51 (d, J = 8.8 Hz, 2H), 7.37 (d, J = 15.8 Hz, 1H), 7.31 – 7.24 (m, 4H), 7.21 (d, J = 15.7 Hz, 1H), 6.96 (d, J = 8.7 Hz, 4H), 6.92 (d, J = 4.4 Hz, 2H), 6.74 (d, J = 8.7 Hz, 2H), 3.88 (s, 6H), 3.08 (s, 6H). ^{13}C NMR (100 MHz, CDCl_3) δ 160.28, 142.35, 134.85, 129.78, 129.35, 128.92, 125.88, 117.02, 114.27, 112.10, 55.37, 40.22. HRMS: m/z : calcd: 624.2598, found: 624.2539 [M+Na] $^+$, Δ =9.4 ppm.

Synthesis of the compound 3:

To a 1 L round-bottomed flask containing 400 mL argon-degassed 1,2-Dichloroethane were added 2,4-Dimethylpyrrole (9.71 mmol, 924.0 mg) and (2) (4.63 mmol, 910.0 mg). The

reaction mixture was refluxed overnight at 60°C. 5 mL of Et₃N and 5 mL of BF₃·OEt₂ were successively added and after 30 min, the reaction mixture was washed three times with water (3 x 100 mL) which was then extracted into the CH₂Cl₂ (3 x 100 mL) and dried over anhydrous Na₂SO₄. The solvent was evaporated and the residue was purified by silica gel column chromatography using 1:1 EtOAc/Hexane as the eluent (703.76 mg, 40%). ¹H NMR (400 MHz, CDCl₃) δ 6.06 (s, 2H), 4.67 (s, 2H), 3.78 – 3.73 (m, 2H), 3.72 – 3.67 (m, 2H), 3.65 – 3.61 (m, 2H), 3.55 – 3.51 (m, 2H), 3.38 (s, 3H), 2.52 (s, 6H), 2.44 (s, 6H). ¹³C NMR (100 MHz, CDCl₃) δ 191.95, 168.29, 155.78, 141.81, 135.99, 132.96, 129.94, 128.49, 127.15, 127.08, 126.88, 122.76, 121.83, 115.25, 115.02, 71.91, 70.96, 70.70, 70.51, 63.92, 59.04, 15.83, 15.38, 14.63, 14.61, 14.58, 11.77. HRMS: *m/z*: calcd: 403.1998, found: 403.1927 [M+Na]⁺, Δ=17.6 ppm.

Synthesis of EUA-4:

(**3**) (0.32 mmol, 122.0 mg) and dimethylaminobenzaldehyde (0.32 mmol, 47.74 mg) were added to a 100 mL round-bottomed flask containing 50 mL benzene and to this solution was added piperidine (0.30 mL) and acetic acid (0.25 mL). The mixture was heated under reflux by using a Dean Stark trap and reaction was monitored by TLC (5% MeOH : 95% DCM). When all the starting material had been consumed, the mixture was cooled to room temperature and solvent was evaporated. Water (100 mL) added to the residue and the product was extracted into the CH₂Cl₂ (3 x 100 mL). Organic phase dried over Na₂SO₄, evaporated and residue was purified by silica gel column chromatography using (5% MeOH : 95% DCM) as the eluent (49.09 mg, %30). ¹H NMR (400 MHz, CDCl₃) δ 7.51 (d, *J* = 8.9 Hz, 2H), 7.47 (d, *J* = 16.4 Hz, 1H), 7.24 (d, *J* = 16.1 Hz, 1H), 6.70 (d, *J* = 8.6 Hz, 2H), 6.68 (s, 1H), 6.06 (s, 1H), 4.70 (s, 2H), 3.79 – 3.75 (m, 2H), 3.73 – 3.69 (m, 2H), 3.67 – 3.62 (m, 2H), 3.56 – 3.52 (m, 2H), 3.39 (s, 3H), 3.04 (s, 6H), 2.55 (d, *J* = 12.4 Hz, 3H), 2.49 (d, *J* = 13.1 Hz, 3H), 2.46 (s, 3H). HRMS: *m/z*: calcd: 534.2698, found: 534.2647 [M+Na]⁺, Δ=9.6 ppm.

Synthesis of EUA-5:

(**3**) (0.39 mmol, 150.0 mg) and dimethylaminobenzaldehyde (0.98 mmol, 147.22 mg) were added to a 100 mL round-bottomed flask containing 50 mL benzene and to this solution was added piperidine (0.50 mL) and acetic acid (0.50 mL). The mixture was heated under reflux by using a Dean Stark trap and reaction was monitored by TLC (5% MeOH : 95% DCM). When all the starting material had been consumed, the mixture was cooled to room temperature and solvent was evaporated. Water (100 mL) added to the residue and the product was extracted into the CH₂Cl₂ (3 x 100 mL). Organic phase dried over Na₂SO₄, evaporated and residue was purified by silica gel column chromatography using (5% MeOH : 95% DCM) as the eluent (87.71 mg, %35). ¹H NMR (400 MHz, CDCl₃) δ 7.58 – 7.49 (m, 6H), 7.21 (d, *J* = 16.1 Hz, 2H), 6.76 – 6.64 (m, 6H), 4.70 (s, 2H), 3.78 – 3.76 (m, 2H), 3.73 – 3.70 (m, 2H), 3.66 – 3.64 (m, 2H), 3.58 – 3.51 (m, 2H), 3.39 (s, 3H), 3.04 (s, 12H), 2.50 (s, 6H). HRMS: *m/z*: calcd: 642.3600, found: 642.3476 [M]⁺, Δ=19.3 ppm.

Measurement of the Constant for Binding of Aβ Aggregates

in Vitro:

For each probe a mixture (100 μL of 10% EtOH) containing EUA-1–5 (final conc. 0–3.75 μM) and Aβ(1–42) aggregates (final conc. 2.2 μM) or BSA (10 μM) was incubated at room temperature for 30 min. Fluorescence intensity of EUA-1–5 at 680, 744, 720, 698, and 784 nm, respectively, was recorded (Ex: 560, 618, 660, 630, and 726 nm for EUA-1–5, respectively). The K_d binding curve was generated by GraphPad Prism 5.0 (GraphPad Software, Inc., La Jolla, CA, USA).

In Vitro Fluorescent Staining of Mouse Brain Sections:

The experiments with animals were conducted in accordance with the institutional guidelines approved by the Kyoto University Animal Care Committee. For each probe, Tg2576 transgenic mouse (female, 28-month-old) was used as the AD model. After the mouse was sacrificed by decapitation, the brain was removed and sliced into serial sections of 10 μm thickness. Each slide was incubated with a 50% EtOH solution of the probes (100 μM). Finally, the sections were washed in 50% EtOH for 1 minute, two times and examined under microscope (BIOREVO BZ-9000, Keyence Corp., Osaka, Japan) equipped with a Texas Red filter set (excitation filter, Ex 540–580 nm; dichroic mirror, DM 595 nm; barrier filter, BA 600–660 nm). The serial sections were also stained with thioflavin S, a pathological dye commonly used for staining Aβ plaques in the brain, and examined using a microscope equipped with a GFP-BP filter set (excitation filter, Ex 450–490 nm; dichroic mirror, DM 495 nm; barrier filter, BA 510–560 nm).

Notes and references

- ⁸⁵ ^aUNAM-National Nanotechnology Research Center, Bilkent University, Ankara 06800, Turkey. Fax: 90 312 266 4068; Tel: 90 312 290 3568; E-mail: eua@fen.bilkent.edu.tr
- ^bDepartment of Patho-Functional Bioanalysis, Graduate School of Pharmaceutical Sciences, Kyoto University, 46-29 Yoshida Shimoadachi-cho, Sakyo-ku, Kyoto 606-8501, Japan.
- ^cDepartment of Chemistry, Bilkent University, Ankara 06800, Turkey.
- † Electronic Supplementary Information (ESI) available: See DOI: 10.1039/b000000x/
- ‡ These two authors made equal contributions.
- 1 (a) R. E. Tanzi, In Scientific American Molecular Neurology; Martin, J. B., Ed.; Scientific American: New York, 1998; (b) M. Goedert and M. G. Spillantini, *Science*, 2006, **314**, 777; (c) C. Mount, C. Downton, *Nat. Med.*, 2006, **12**, 780; (d) S. Gandy, *Nature*, 2011, **475**, S15; (e) A. Abbott, *Nature*, 2011, **475**, S2.
- 2 R. Luengo-Fernandez, J. Leal and A. Gray, Dementia 2010; Health Economics Research Centre: Oxford, 2010.
- 3 (a) D. J. Selkoe, *Physiol. Rev.*, 2001, **81**, 741; (b) J. Hardy and D. J. Selkoe, *Science*, 2002, **297**, 353; (c) C. Haass and D. J. Selkoe, *Nat. Rev. Mol. Cell Biol.*, 2007, **8**, 101; (d) G. B. Irvine, O. M. A. El-Agnaf, G. M. Shankar and D. M. Walsh, *Mol. Med.*, 2008, **14**, 451; (e) D. J. Selkoe, *Nat. Med.*, 2011, **17**, 1060; (f) I. W. Hamley, *Chem. Rev.*, 2012, **112**, 5147.
- 100 4 (a) I. Melnikova, *Nature Rev. Drug Discovery*, 2007, **6**, 341; (b) L. Mucke, *Nature (London)*, 2009, **461**, 895.
- 5 (a) J. T. Jarrett, E. P. Berger and P. T. Lansbury, *Biochemistry*, 1993, **32**, 4693; (b) P. T. Lansbury and H. A. Lashuel, *Nature*, 2006, **443**, 774.
- 115 6 W. R. Markesbery, *Free Radical Biol. Med.*, 1997, **23**, 134.
- 7 C. R. Jack, D. S. Knopman, W. J. Jagust, L. M. Shaw, P. S.

- Aisen, M. W. Weiner, R. C. Petersen and J. Q. Trojanowski, *Lancet Neurol.*, 2010, **9**, 119.
- 8 H. Hampel, R. Frank, K. Broich, S. J. Teipel, R. G. Katz, J. Hardy, K. Herholz, W. Bokde, F. Jessen, Y. C. Hoessler, W. R. Sanhai, H. Zetterberg, J. Woodcock, and K. Blennow, *Nature Rev. Drug Discovery*, 2010, **9**, 560.
- 9 (a) M. Ono, H. Watanabe, H. Kimura and H. Saji, *ACS Chem. Neurosci.*, 2012, **3**, 319; (b) M. Hintersteiner, A. Enz, P. Frey, A.-L. Jatton, W. Kinzy, R. Kneuer, U. Neumann, M. Rudin, M. Staufenbiel, M. Stoeckli, K.-H. Wiederhold and H.-U. Gremlich, *Nat. Biotechnol.*, 2005, **23**, 577; (c) H. Watanabe, M. Ono, K. Matsumura, M. Yoshimura, H. Kimura and H. Saji, *Mol. Imaging*, 2013, **12**, 338; (d) C. Ran, X. Xu, S. B. Raymond, B. J. Ferrara, K. Neal, B. J. Bacskai, Z. Medarova and A. Moore, *J. Am. Chem. Soc.*, 2009, **131**, 15257; (f)
- 10 E. E. Nesterov, J. Skoch, B. T. Hyman, W. E. Klunk, B. J. Bacskai and T. M. Swager, *Angew. Chem., Int. Ed. Engl.* 2005, **44**, 5452.
- 11 (a) H. Choi, J. H. Lee and J. H. Jung, *Analyst*, 2014, **139**, 3866; (b) O. A. Bozdemir, R. Guliyev, O. Buyukcakil, S. Selcuk, S. Kolemen, G. Gulseren, T. Nalbantoglu, H. Boyaci and E. U. Akkaya, *J. Am. Chem. Soc.*, 2010, **132**, 8029; (c) R. Guliyev, S. Ozturk, Z. Kostereli and E. U. Akkaya, *Angew. Chem. Int. Ed.*, 2011, **50**, 9826; (d) N. Boen, V. Leen and W. Dehaen, *Chem. Soc. Rev.*, 2012, **41**, 1130; (e) O. A. Bozdemir, F. Sozmen, R. Guliyev, Y. Cakmak and E. U. Akkaya, *Org. Lett.*, 2010, **12**, 1400; (f) L.-Ya. Niu, Y.-S. Guan, Y.-Z. Chen, L.-Z. Wu, C.-H. Tung and Q.-Z. Yang, *J. Am. Chem. Soc.*, 2012, **134**, 18928; (g) T. Ozdemir, F. Sozmen, S. Mamur, T. Tekinay and E. U. Akkaya, *Chem. Commun.*, 2014, **50**, 5455.
- 12 (a) S. G. Awuah and Y. You, *RSC Adv.*, 2012, **2**, 11169; (b) Y. Cakmak, S. Kolemen, S. Duman, Y. Dede, Y. Dolen, B. Kilic, Z. Kostereli, L. T. Yildirim, A. L. Dogan, D. Guc, and E. U. Akkaya, *Angew. Chem., Int. Ed.*, 2011, **50**, 11937; (c) A. Kamkaew, S. H. Lim, H. B. Lee, L. V. Kiew, L. Y. Chung and K. Burgess, *Chem. Soc. Rev.*, 2013, **42**, 77.
- 13 (a) Y.-S. Yen, H.-H. Chou, Y.-C. Chen, C.-Y. Hsu and J. T. Lin, *J. Mater. Chem.*, 2012, **22**, 8734; (b) S. Kolemen, Y. Cakmak, S. E. Ela, Y. Altay, J. Brendel, M. Thelakkat and E. U. Akkaya, *Org. Lett.*, 2010, **12**, 3812; (c) A. Hagfeldt, G. Boschloo, L. Sun, L. Kloo and H. Pettersson, *Chem. Rev.*, 2010, **110**, 6595; (d) S. Kolemen, O. A. Bozdemir, Y. Cakmak and E. U. Akkaya, *Chem. Sci.*, 2011, **2**, 949.
- 45 14 (a) R. Ziessel and A. Harriman, *Chem. Commun.*, 2011, **47**, 611; (b) O. A. Bozdemir, Y. Cakmak, F. Sozmen, T. Ozdemir, A. Siemiarzuck and E. U. Akkaya, *Chem. Eur. J.*, 2010, **16**, 6346; (c) G. Ulrich, R. Ziessel and A. Harriman, *Angew. Chem., Int. Ed.*, 2008, **47**, 1184; (d) F. Sozmen, B. S. Oksal, O. A. Bozdemir, O. Buyukcakil and E. U. Akkaya, *Org. Lett.*, 2012, **14**, 5286; (e) S. Atilgan, T. Ozdemir and E. U. Akkaya, *Org. Lett.*, 2010, **12**, 4792.
- 15 (a) A. Loudet and K. Burgess, *Chem. Rev.*, 2007, **107**, 4891; (b) S. Atilgan, T. Ozdemir and E. U. Akkaya, *Org. Lett.*, 2008, **10**, 4065; (c) W. Zhao and E. M. Carreira, *Angew., Chem. Int. Ed.*, 2005, **44**, 1677.
- 16 (a) S. Zhu, J. Zhang, G. Vegesna, A. Tiwari, F.-T. Luo, M. Zeller, R. Luck, H. Li, S. Green and H. Liu, *RSC Adv.*, 2012, **2**, 404; (b) O. Buyukcakil, O. A. Bozdemir, S. Kolemen, S. Erbas and E. U. Akkaya, *Org. Lett.*, 2009, **16**, 4644.
- 60
- 65

TOC Graph

